Graphical Abstract

What price to pay? Auto-tuning a building MPC controller for optimal economic cost

Jiarui Yu , Jicheng Shi, Wenjie Xu, Colin N. Jones

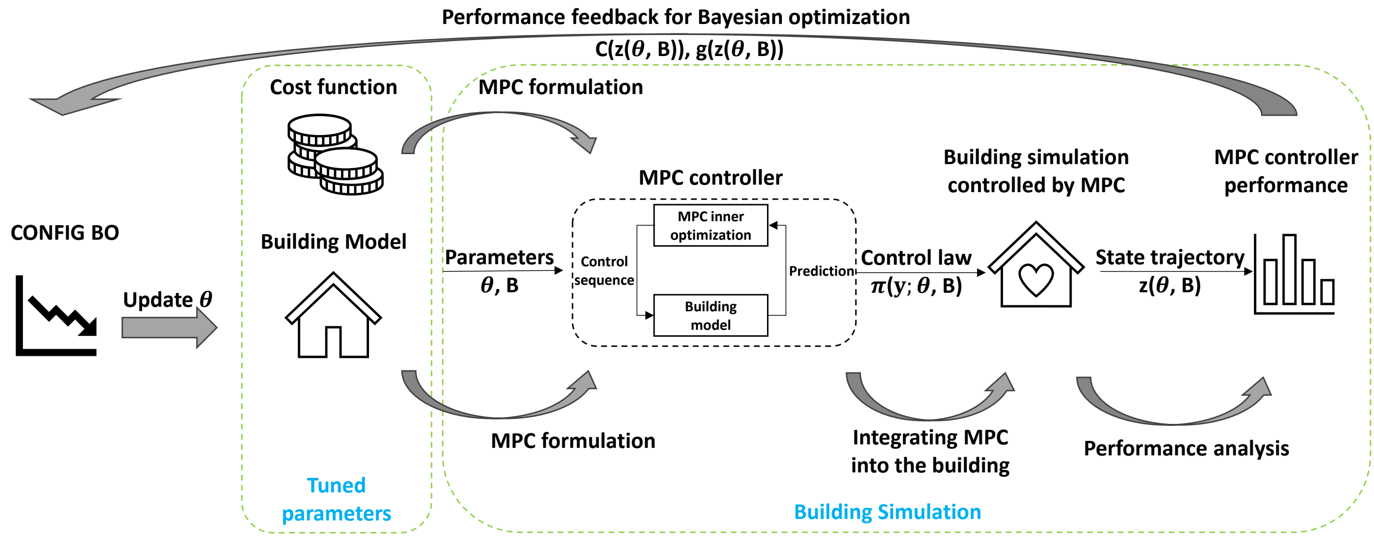

Highlights

What price to pay? Auto-tuning a building MPC controller for optimal economic cost

Jiarui Yu , Jicheng Shi, Wenjie Xu, Colin N. Jones

- Constrained Bayesian Optimization of MPC controller in building control.
- It yields superior performance compared to a computationally intensive MPC.
- Guidance on selecting from different electricity plans under customized constraints.
- Up to 20% monthly saving compared with the worst contract.

What price to pay? Auto-tuning a building MPC controller for optimal economic cost

Jiarui Yu [a,1], Jicheng Shi[a,1], Wenjie Xu[a,1,*], Colin N. Jones[a]

[a] *Laboratoire d'Automatique, EPFL, 1015 Lausanne, Switzerland*

Abstract

Urbanization and rising energy demand make efficient building control essential. Demand-side management (DSM) programs have been introduced to help balance consumption and grid stability but also introduce complexity, making it harder for consumers to identify the most cost-effective options. To maximize savings while maintaining comfort, buildings must adapt to fluctuating energy prices. Traditional rule-based control struggles with such variability, while model predictive control (MPC) offers a more flexible and predictive solution. However, MPC's performance depends on well-tuned hyperparameters, which vary across DSM programs. Conventional controller design often overlooks this, leading to suboptimal performance due to environmental disturbances, modeling inaccuracies, and poor adaptation to pricing schemes, ultimately increasing costs.

To address these challenges, we propose a performance-oriented MPC tuning method using the constrained Bayesian optimization algorithm, CONFIG. This approach ensures global optimality while satisfying black-box constraints. It efficiently identifies the optimal costs and corresponding hyperparameters, providing consumers with insights into DSM program selection and controller configuration. We validated the method through a case study on the BOPTEST building simulation platform. An MPC controller based on a linear data-driven model was designed to reduce commissioning costs and improve computational efficiency. It was then optimized to match the performance of a computationally intensive MPC controller. Results show that the optimized MPC can reduce household electricity costs by up to 26.90% compared to a rule-based controller under the same constraints. Additionally, an analysis of 12 real electricity contracts in Belgium found that selecting the most cost-effective option can lower monthly bills by up to 20.18%, highlighting the impact of contract selection.

Keywords: Demand-side management, Performance optimization, Constrained Bayesian optimization, Model predictive control

1. Introduction

Rapid urbanization and population growth have significantly increased global energy demand and carbon emissions, placing immense pressure on the environment and energy infrastructure. Buildings account for about 34% of global energy use [1], with nearly half consumed by HVAC systems [2]. To enhance grid stability and operational efficiency, price-based demand-side management (DSM) programs—such as time-of-use, real-time, and critical peak pricing—have been widely implemented. These programs encourage consumers to shift energy usage in response to fluctuating electricity prices, thereby helping balance grid load and improve operational efficiency.

Despite these benefits, DSM programs introduce challenges for consumers and building operators. They must select among a wide range of electricity contracts with different rates, peak pricing structures, and time-based tariffs [3]. Selecting the most cost-effective contract is difficult, especially when combined with the need to optimize building control strategies that minimize costs while maintaining occupant comfort. Existing services that support contract selection guidance [4, 5] typically analyze historical data to predict electricity usage patterns [6] and recommend suitable contracts. However, selecting the right contract alone is not sufficient. Greater cost savings can be achieved by adapting electricity consumption through controllers designed for specific pricing structures [7]. Implementing such an approach requires advanced control strategies, but traditional rule-based controllers often struggle with the complexities of dynamic pricing schemes [8].

Model Predictive Control (MPC) has emerged as a promising solution to these challenges, leveraging its ability to predict future energy prices and building thermal dynamics [9]. This predictive capability enables superior performance and greater robustness in managing buildings under various DSM billing contracts, such as time-of-use pricing [10], critical peak pricing [11], and real-time pricing schemes [12], by allowing the controller to anticipate cost variations and adjust energy use accordingly. For example, Yang et al. [12] developed an MPC controller designed for highly dynamic electricity prices in demand-responsive building control. Compared to two conventional controllers, their MPC implementation reduced heating energy consumption by up to 13.8% and electricity costs by up to 70%, all while maintaining acceptable comfort levels. However, MPC's effectiveness depends on carefully selecting cost and constraint functions, as well as key parameters such as model structure and coefficients, to achieve optimal performance [13].

Yet, the conventional MPC design process typically follows two separate stages [14]: building model construction and con-

[*] Corresponding author at: Laboratoire d'Automatique, Swiss Federal Institute of Technology Lausanne (EPFL), 1015 Lausanne, Switzerland. E-mail address: wenjie.xu@epfl.ch (W. Xu).

[1] The first three authors contribute equally to this work.

Nomenclature

Abbreviations		$\mathcal{Y}$	Constraint set for indoor temperature
ANN	Artificial Neural Network	J	Performance objective
ARX	AutoRegressive model with eXogenous inputs	Θ	Sample sequence
BO	Bayesian Optimization	θ	Tuning parameters in CONFIG algorithm
CDF	Cumulative Distribution Function	$A(q)$	Coefficient for previous output
CONFIG	Constrained Efficient Global Optimization	K	Total number of iterations in CONFIG
DSM	Demand-side Management	N	Total time steps
GA	Genetic Algorithm	n	Total number of DSM programs to choose from
HVAC	Heating, Ventilation, and Air Conditioning	R	Linear penalty coefficient for heating power
i.i.d	Independent and identically distributed	S	Penalty coefficient for slack variable
MIQP	Mix Integer Quadratic Programming	t_d	Time delay
ML	Machine Learning	u	Input heat pump power
MPC	Model Predictive Control	y	Indoor Temperature
NN	Neural Network	y_{ref}	Temperature setpoint
PMV	Predicted Mean Vote	***Subscripts***	
RL	Reinforcement Learning	0	Measurement of objective in CONFIG
Variables		1	Measurement of constraint in CONFIG
$\beta^{1/2}$	Weighting parameter in CONFIG	$config$	For CONFIG problem
g	Performance constraint	k	Iteration steps for CONFIG
ϵ	Slack variable for temperature constraints	mpc	For MPC problem
λ	Gaussian process noise variance	t	Index of time steps for building model
$\mathcal{U}$	Constraint set for control input		

troller design. The modeling stage aims to accurately predict building dynamics. To reduce engineering effort across diverse buildings, researchers have explored a variety of modeling techniques. Resistor-Capacitor (RC) models have been used for their physical interpretability and simplicity [15, 16]. Behavioral modeling approaches capture occupancy and usage patterns directly from data [17]. Gaussian Process models offer probabilistic predictions with quantified uncertainty [18], while Neural Networks enable high-capacity, data-driven modeling of complex thermal dynamics [19–21]. These methods construct models from building performance data by minimizing prediction errors. After model construction, MPC controllers are designed with objectives and constraints tailored to different electricity billing contracts [12], stochastic environments [22], and dynamic estimates and predictions [23]. However, real building systems are subject to various disturbances and complex nonlinear components, making it inherently difficult to perfectly estimate predictive models or control objectives. For instance, data-driven models often suffer from underfitting or overfitting [24], leading to poor generalization in real-world scenarios. This estimation mismatch complicates control decisions, especially when different MPC components are tuned separately. Without a joint tuning approach, misalignment between model predictions and control objectives can degrade overall performance. Research shows that higher prediction accuracy does not necessarily improve control outcomes, as models may fail to generalize [25], noises and uncertainties [26], or unmodeled dynamics [27]. To address these challenges, a joint tuning approach that optimizes all significant hyperparameters is essential for ensuring reliable and effective real-world performance.

Several studies have explored performance-oriented controller design for building control. For example, [28] applied a primal-dual contextual Bayesian optimization method to tune a PI controller, reducing energy use while maintaining comfort. Similarly, [29] used Bayesian optimization for HVAC setpoint tuning, and [30] employed an iterative optimization technique to determine optimal deployment strategies for multi-energy storage at the cluster level. However, these works did not use MPC and therefore lacked the predictive capabilities necessary for DSM pricing environments. More recent efforts have investigated MPC tuning. [31] used a heuristic search algorithm to tune the LSTM-based MPC controller, while [32] applied sample average approximation as a surrogate to evaluate controller performance under uncertainty. These approaches, however, may struggle with local minima despite using multi-start strategies. Bayesian optimization has been applied to mitigate this issue and is effective for optimizing black-box objectives, such as total energy cost [33]. However, most existing BO-based MPC methods do not support black-box constraints [33], such as long-term comfort violation limits, or require manually identified reference models [34], limiting their scalability.

This limitation is particularly critical in DSM-based building control, where the goal is to minimize electricity cost under complex pricing contracts while maintaining long-term comfort. Due to model inaccuracies and limited prediction horizons, MPC can only approximate these long-term closed-loop outcomes. In practice, comfort satisfaction can only be evaluated through extended simulation or deployment, making them black-box functions in the control design process. Although constrained Bayesian optimization techniques—such as CONFIG [35]—can handle black-box objectives and constraints, their application to MPC tuning for DSM-based building control remains largely unexplored. This raises a critical question: can such methods reliably deliver cost-effective and comfort-compliant control across diverse real-world electricity contracts?

To address this gap, we propose a performance-oriented MPC design framework based on CONFIG [35], an efficient constrained Bayesian optimization method that ensures global optimality while satisfying black-box constraints. The proposed framework is validated through a complex building control task involving various DSM electricity contracts. The key contributions of this work are summarized as follows:

1. An MPC design framework is proposed for building control, which leverages CONFIG to automatically tune hyperparameters under black-box objectives and constraints, providing global optimality guarantees.

2. The framework was validated by optimizing an MPC based on linear data-driven model for efficient building control. The optimized MPC achieved superior performance compared to a computationally intensive MPC.

3. In the case study, the performance of the optimized MPC controller was evaluated under 12 real billing contracts in Belgium, as shown in Table 5, offering guidance for contract selection. The comfort constraint, defined using a cumulative distribution function, was satisfied under all contract scenarios in the closed loop.

2. Problem Statement

This paper presents a hyperparameter offline tuning approach to optimize the performance of an MPC building controller under various electricity billing contracts. Let θ be a vector of tuning parameters for an MPC controller and $\mathcal{B} = \{B_1, B_2, \ldots, B_n\}$ be the set of potential electricity contracts. The total electricity cost over a considered time period T is denoted as $C^\star$ and the contract selection problem to be solved is

$$C_{\min} = \min_{B \in \mathcal{B}} C^\star(B) \tag{1}$$

We define the control law as $\pi(y; B, \theta)$, which is a function of the state y and is parameterized by the energy contract B and the controller parameters θ. Given the control law π, we define the closed-loop state and input trajectories as $\mathbf{z}(B, \theta) = \{(y_0, u_0), \ldots, (y_T, u_T)\}$ over the tuning period T. The details of the control law implementation as a generic MPC controller are given in section. 4.3.

We then define the *controller tuning problem* as

$$C^\star(B) = \min_{\theta} C(\mathbf{z}(\theta, B), B) \tag{2}$$

$$\text{s.t. } g(\mathbf{z}(\theta, B)) \leq 0 \tag{3}$$

where $C(\mathbf{z}, B)$ is the total financial cost of the trajectory $\mathbf{z}$ under the contract B, and g measures the comfort of the occupants of the building.

3. Methodology

3.1. Overview

First, historical data from a building controlled by a local controller is collected to identify a parametric building model. Notably, the local controller can be arbitrary, and the collected data is used solely to model building dynamics, not to predict electricity usage patterns. Next, as shown in Fig. 1, an MPC controller is formulated with a predefined cost function (objective) and constraint functions, which are then integrated into the building simulator. This study focuses on offline tuning problems, with online deployment reserved for future work. Third, building simulation data over the same time span is used to evaluate the MPC controller's performance. Key metrics, such as total electricity bills and indoor thermal comfort, are input into the CONFIG algorithm, which then determines new parameters for the MPC controller, forming an optimization cycle. Our performance-oriented optimization approach leverages digital twin technology [36], enabling detailed simulations and modeling that provide a reliable representation of real building behavior without disrupting or altering the physical system.

With this framework, the optimal hyperparameter set and the corresponding electricity cost for a given billing contract can be obtained efficiently. Finally, by comparing the optimal results of various contracts, we provide guidance for consumers to select the most economical option and offer tailored control recommendations.

3.2. CONFIG algorithm

Before deploying controllers in buildings, the relationships among hyperparameters, objectives, and constraints are often unclear. Consequently, optimizing control parameters becomes a black-box problem, typically solved using Bayesian Optimization (BO). BO employs probabilistic surrogate models, such as Gaussian processes, to approximate objectives, enabling efficient exploration of complex, high-cost parameter spaces. By strategically selecting the next parameter set based on prior observations and acquisition functions, BO achieves strong performance with minimal evaluations.

Within the BO framework, CONFIG [35] outperforms other methods by effectively balancing exploration, exploitation, and constraint satisfaction. It provides theoretical guarantees for global convergence while modeling black-box constraints, enabling compliance with complex consumer requirements that are challenging to embed in controllers. By ensuring global optimality, CONFIG identifies the best parameter combination and minimizes costs under specific billing contracts. For these reasons, we selected CONFIG as the optimization algorithm for this work.

Fig. 2 illustrates the CONFIG algorithm using a simple one-dimensional example. In a building control optimization problem, each point represents a vector of tuning parameters. This point is fed into a black-box function, which, in this study, is

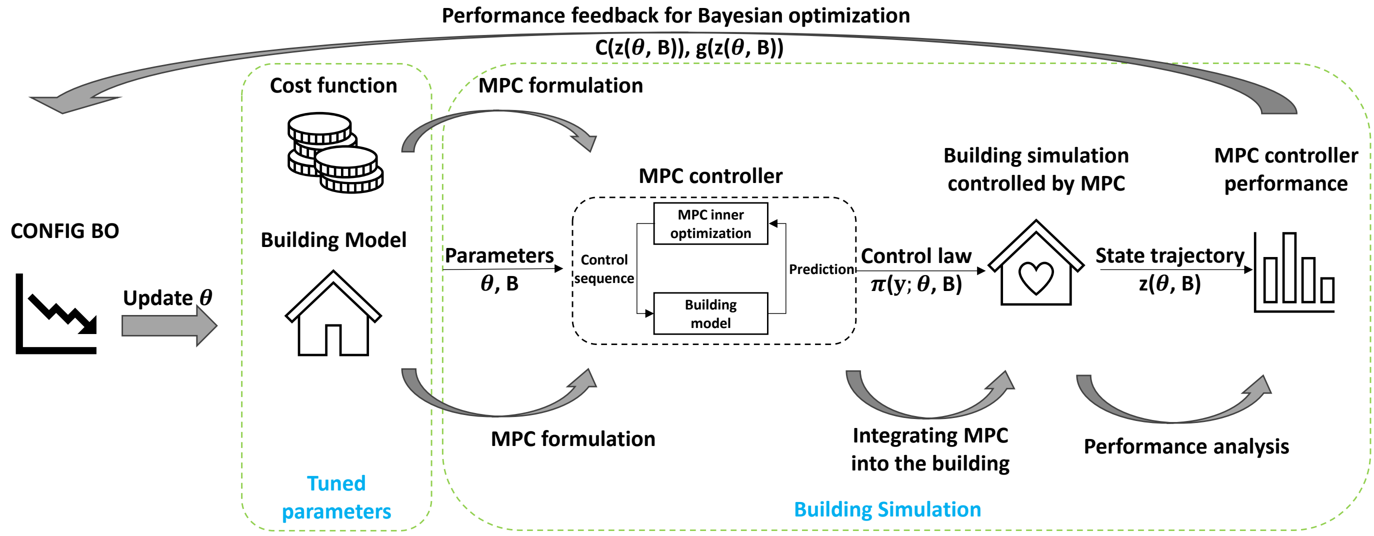

Figure 1: An overview of the approach for developing the performance-oriented MPC controller tuning in building control

the building simulation platform. Performance metrics are derived from the black-box function's outputs and, along with the corresponding points, form the sampled data. A Gaussian process (GP) is applied to the sampled data to surrogate the black-box function's behavior, providing a mean (the blue line in the upper figure) and confidence interval (the blue area in the upper figure). CONFIG selects the next sampling point using the lower confidence bound (red line) by identifying the point with the lowest performance metric. This point is then evaluated by the black-box function, initiating a new iteration. The process repeats until reaching a predefined number of iterations. While CONFIG incorporates constraints, they are not depicted in this example. Further details are provided in sections 3.3 and 3.4.

3.3. Gaussian process regression

For CONFIG BO in our paper, the unknown objective function is $C(z(\theta, B), B)$ and the unknown constraint is $g(z(\theta, B))$. Gaussian process surrogate functions are employed to model their behaviors. Specifically, we introduce a Gaussian process $\mathcal{GP}(0, k_i(\cdot, \cdot)), i \in \{0\} \cup \{1\}$ as well as an i.i.d Gaussian zero-mean noise model with noise variance λ. Let $h_{0,k}$ denote the measurement of the objective $C(z(\theta_k, B), B)$ with sample θ_k at iteration k. Let Θ_k denote the sample sequence $(\theta_1, \theta_2, \ldots, \theta_k)$. To be noted, this measurement is influenced by the independently distributed σ_0 sub-Gaussian noise introduced in the Gaussian zero-mean noise model. Similarly, for the measurement of the constraint $g(z(\theta_k, B))$, we introduce $h_{1,k}$ which is also corrupted by sub-Gaussian noise. For the Gaussian process, the following functions for θ and θ' are introduced,

$$\mu_{0,k}(\theta) = k_0(\theta_{1:k}, \theta)^\top (K_{0,k} + \lambda I)^{-1} h_{0,1:k} \tag{4a}$$

$$k_{0,k}(\theta, \theta') = k_0(\theta, \theta') - k_0(\theta_{1:k}, \theta)^\top (K_{0,k} + \lambda I)^{-1} k_0(\theta_{1:k}, \theta') \tag{4b}$$

$$\sigma^2_{0,k}(\theta) = k_{0,k}(\theta, \theta) \tag{4c}$$

where $k_0(\theta_{1:k}, \theta) = [k_0(\theta_1, \theta), k_0(\theta_2, \theta), \ldots, k_0(\theta_k, \theta)]^\top$, $K_{0,k} = (k_0(\theta, \theta')_{\theta, \theta' \in \Theta_k})$ and $h_{0,1:k} = [h_{0,1}, h_{0,2}, \ldots, h_{0,k}]^\top$. Through the same approach, $\mu_{1,k}(\cdot)$, $k_{1,k}(\cdot)$ and $\sigma_{1,k}(\cdot)$ can be obtained. With these Gaussian process posterior distribution functions, the acquisition function in CONFIG algorithm can be solved and then the optimal next sampling parameter set is obtained.

3.4. CONFIG for controller tuning

With the preparations outlined in section. 3.3, the performance oriented optimization is applied as illustrated in Algorithm. 1. A weighting parameter $\beta^{1/2}_{i,k}$ is introduced to balance the decision of whether to explore further unknown area or to exploit at the current spot. K represents the total iterations of the CONFIG algorithm and Θ denotes the space of hyperparameters to be explored and evaluated. Then the algorithm posts an auxiliary problem as shown in Line. (5) of the Algorithm. 1. Specifically, rather than directly solving the constrained minimization problem with unknown objective and constraints, the algorithm solves the auxiliary problem with the original objective and constraints replaced by their lower confidence bound surrogates. Before the auxiliary problem is solved, its feasibility is verified as shown in Line. 3. If deemed infeasible, an infeasibility warning for the original problem is declared. A theoretical guideline for selecting the value of $\beta^{1/2}_{i,k}$ to guarantee the global optimality is introduced and proved in [35].

Algorithm 1 CONFIG for Controller Tuning

1: **for** $k \in [K]$ **do**
2: **if** $\min_{\theta \in \Theta}(\mu_{1,k}(\theta) - \beta^{1/2}_{1,k}\sigma_{1,k}(\theta)) > 0$ **then**
3: **Declare infeasibility**.
4: **end if**
5: Update controller parameters with

$$\theta_k \in \arg\min_{\theta \in \Theta} \quad \mu_{0,k}(\theta) - \beta^{1/2}_{0,k}\sigma_{0,k}(\theta)$$

$$\textbf{subject to } \mu_{1,k}(\theta) - \beta^{1/2}_{1,k}\sigma_{1,k}(\theta) \le 0, .$$

6: Run building simulation to get measurements of $C(z(\theta_k, B), B)$ and $g(z(\theta_k, B))$.
7: Update Gaussian process posterior mean and covariance with the new evaluations added.
8: **end for**

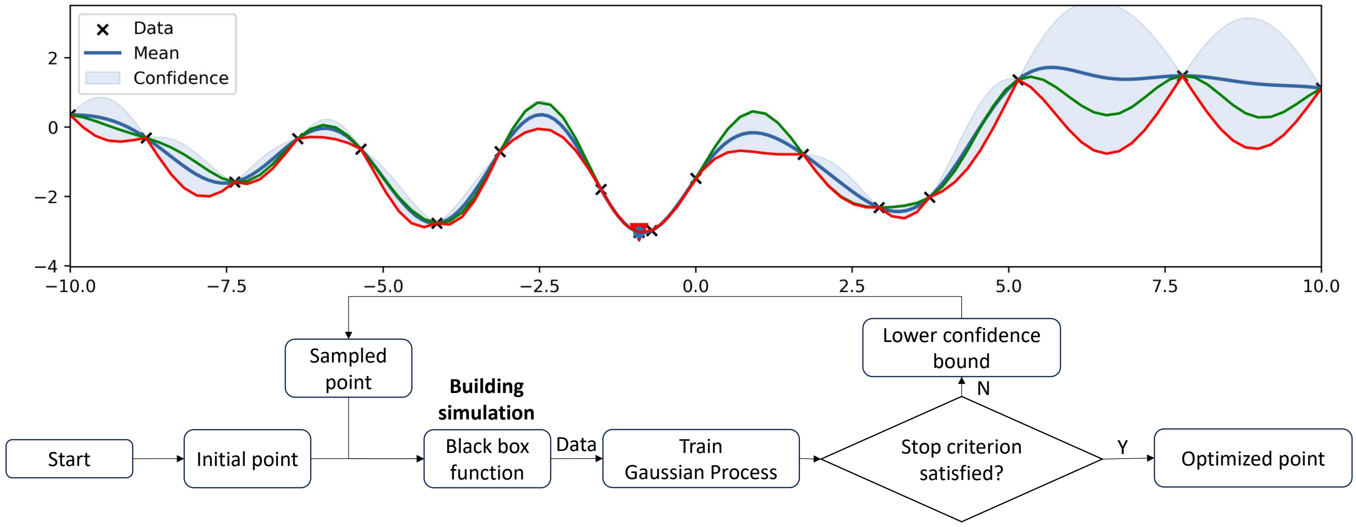

Figure 2: An overview of the CONFIG Bayesian Optimization method. The *point* in the flow chart refers to a vector composed of tuning parameters. *Data* is a *point* together with its performance metric obtained from the black-box function. With obtained *Data*, CONFIG utilized Gaussian progress (GP) to surrogate black-box function behavior with *Mean* and *Confidence*. CONFIG computes the lower confidence bound of the GP and choose the next point with the smallest performance metric value on the lower confidence bound.

4. Case study: basic settings

4.1. Simulation platform

The simulation platform selected for this work is the Building Optimization Performance Tests (BOPTEST [37]). Specifically, the testcase *bestest_hydronic_heat_pump* was chosen for this case study. This represents a residential building located in Brussels, Belgium, modeled as a single thermal zone following the BESTEST case 900 test case parameters. The residence is heated by a 15 kW air-to-water modulating heat pump, which extracts heat from the surrounding air to warm a floor heating system. The heat pump's evaporator is assisted by a fan, and a circulation pump transfers water from the heat pump to the floor during operation. Further details are provided in Table. 1. The power of the heat pump is regulated by a modulated heat pump signal between 0 and 1, with no functionality at 0 and full capacity at 1.

4.2. Linear data-driven building modeling

To enhance MPC controller performance, the building model must accurately capture building dynamics. While various modeling techniques exist, we implemented a linear data-driven AutoRegressive model with eXogenous inputs (ARX) for two key reasons.

First, data-driven models offer greater adaptability and lower commissioning costs [38, 39]. Developing physics-based models requires extensive knowledge of thermal properties, HVAC dynamics, and occupancy behavior, making them time-consuming and computationally demanding. In contrast, data-driven models learn system behavior from historical sensor data, reducing manual effort. While physics-based models provide interpretability, their simplifications can introduce inaccuracies. Properly trained data-driven models can achieve comparable predictive accuracy at significantly lower costs [40]. Additionally, they adapt to changes in building usage, weather, and equipment performance, enhancing long-term control accuracy [41].

Second, linear models are widely used in the building sector for MPC due to their effectiveness and efficiency [42]. For example, [43] demonstrated that a physics-informed linear regression model outperformed ML models in real-world applications. In buildings equipped with heat pumps, linear models have shown strong control performance in field demonstrations [17, 39]. In addition, [44] compared various models using the *bestest_hydronic_heat_pump* test case and found that a linear data-driven model achieved comparable performance to a gray-box model [45] and other nonlinear methods. Linear models also require less data, reducing commissioning costs compared to nonlinear approaches. Moreover, MPC based on a linear model requires low computational resources, making it practical for daily household energy management. A detailed comparison of computational requirements is provided in section 4.3.

Given the high cost of advanced controllers for typical households and the adequate expressive capability of linear models, a linear data-driven ARX model was chosen for the MPC prediction model, as shown in Eq. (5b). Components of the ARX model are detailed in section. 4.3.

4.3. MPC controller design

Basic Configuration To focus the MPC controller on reducing the final electricity cost, we formulate it in an economic way. First, at time step t, we define p_t as the electricity price per kilowatt, y_t to be the indoor temperature and u_t to be the control input, i.e. modulated heat pump signal. Then, with ARX model coefficients $A(q)$ and $B(q)$, the building model in MPC controller can be formulated as Eq. (5b). u_{ARX} is the input for the ARX model, which is a vector composed of heat pump input u, outdoor temperature and solar radiation. t_d is a constant time delay for ARX model. For the MPC constraints, we introduce $\mathcal{Y}$ and $\mathcal{U}$ to be the feasible set of the t^{th} step indoor temperature y_t and control input u_t respectively, as shown in Eq. (5c) and (5e). In this case study, modulated heat pump input is set to be

Table 1: Building information, HVAC, schedule and tariff summary

	Description
Building information	1. A simplified residential dwelling for 5 occupants 2. A single zone with a floor plan of 12 by 16 meters and a height of 2.7 m 3. 12 rooms in the building 4. Exterior walls: consist of wood siding, insulation and concrete block 5. A single window of $24m^2$
HVAC	1. Air-to-water modulating heat pump of 15 kW nominal heating capacity 2. Floor heating system with water as working fluid 3. Modulating input signal: 0 (not working) to 1 (working at maximum capacity)
Schedule	1. Occupied by 5 people before 7 am and after 8 pm each weekday 2. Occupied full time during weekends

between 0 and 1, while we set an upper bound u_{max} to limit the power of the heat pump and to reduce the peak power. We set different temperature constraints for occupied and unoccupied scenarios. In this way, $[T_{lb}^{occupy}, T_{ub}^{occupy}]$ and $[T_{lb}^{unoccupy}, T_{ub}^{unoccupy}]$ are two constraints for indoor temperature in occupied hours and unoccupied hours respectively as shown in Fig. 3. To ensure feasibility, we use a slack variable, ϵ, for soft constraints. R and S refer to the penalty coefficients for the linear and slack variable penalties, respectively. Finally, the basic QP MPC formulation is shown as Eq. (5), where $\mathbb{B}$ is a unit ball in an appropriate norm. It is evident that since all the elements are parametric, the performance of the MPC controller can be regarded as a black-box function of the variables including $\mathcal{U}$, R, $A(q)$, $B(q)$ and etc.

$$\textbf{QP:} \quad J_{mpc}^{*}(y, u) = \min_{y,u} \sum_{t=0}^{N-1} Rp_t u_t + \epsilon_t' S \epsilon_t \tag{5a}$$

subject to:

$$A(q)y(t) = B(q)u_{ARX}(t - t_d) \tag{5b}$$

$$y_t \in \mathcal{Y} \oplus \epsilon\mathbb{B} \tag{5c}$$

$$\mathcal{Y} = [T_{lb}^{occupy}, T_{ub}^{occupy}] \text{ if } t \text{ in occupied hours}$$

$$\mathcal{Y} = [T_{lb}^{unoccupy}, T_{ub}^{unoccupy}] \text{ otherwise} \tag{5d}$$

$$u_t \in \mathcal{U} \tag{5e}$$

$$\mathcal{U} = [0, u_{max}] \tag{5f}$$

Minimum Operating Power Issue After integrating the basic QP MPC into the building simulation, a minimum operating power (MOP) issue was identified as shown in Fig. 4. When the modulated input signal is zero, the electricity power remains at zero. However, when the input signal increases slightly above zero, fundamental components such as fans of the heat hump, would activate, resulting in a spike in the electricity power to approximately 1 kW. Unlike bang-bang control, which only uses binary inputs and avoids intermediate states, a typical MPC may output small non-zero inputs. This leads to frequent switching from 0 to low values, as seen in Fig. 4. These small activations trigger the heat pump unnecessarily, incurring system operating with a minimum power without delivering significant thermal output, thus reducing overall system efficiency. As a periodic pseudorandom binary sequence (PRBS) signal is employed to stimulate the building behavior for building model identification, the ARX model is unable to capture the associated minimum operating power implications. Consequently, this issue must be addressed at the control level.

MPC Design We set up a MPC targeted to solve the MOP issue as shown in Eq. 6. Instead of directly input u_t to the simulator, we have introduced an extra variable called $u_{mpc,t}$ for time step t. The mapping from u_t to $u_{mpc,t}$ is defined by function $mask()$. Then we introduce two approximation methods to include MOP issue in the MPC as shown in Table. 2.

$$\textbf{MOP:} \quad J_{mpc}^{*}(y, u) = \min_{y,u,\alpha} \sum_{t=0}^{N-1} Rp_t P_{elec,t} + \epsilon_t' S \epsilon_t \tag{6a}$$

subject to:

$$(5b), (5c), (5d) \tag{6b}$$

$$u_t, P_{elec,t} \in \text{U} \tag{6c}$$

$$u_{mpc,t} = mask(u_t) \tag{6d}$$

For the MIQP MPC case, the relationship between the modulated signal, u, and the real electricity power, P_{elec}, can be approximated as a mixed-integer constraint, i.e. $P_{elec} = \phi \cdot u + \gamma$, where γ denotes the system minimum operating power and ϕ represents the power to increase per unit of u increase. This formulation introduces integer variables, making the control problem a Mixed-Integer Quadratic Programming (MIQP) problem. A binary variable α (which can be either 0 or 1) is used to introduce switching behaviors or on-off decisions. For instance, constraints like $0 \leq u_t \leq \alpha u_{max}$ ensure that u_t and u_{mpc} are both zero when α is zero, effectively turning off certain control actions. These mechanisms allow the optimization to incorporate both continuous control inputs and discrete decision-making, enhancing the flexibility and applicability of the control strategy. To be noted, as the identification of the ARX model remains the same, u_{ARX} is still composed of the modulated heat pump input, u_t, and the other environmental variables. For convenience, the

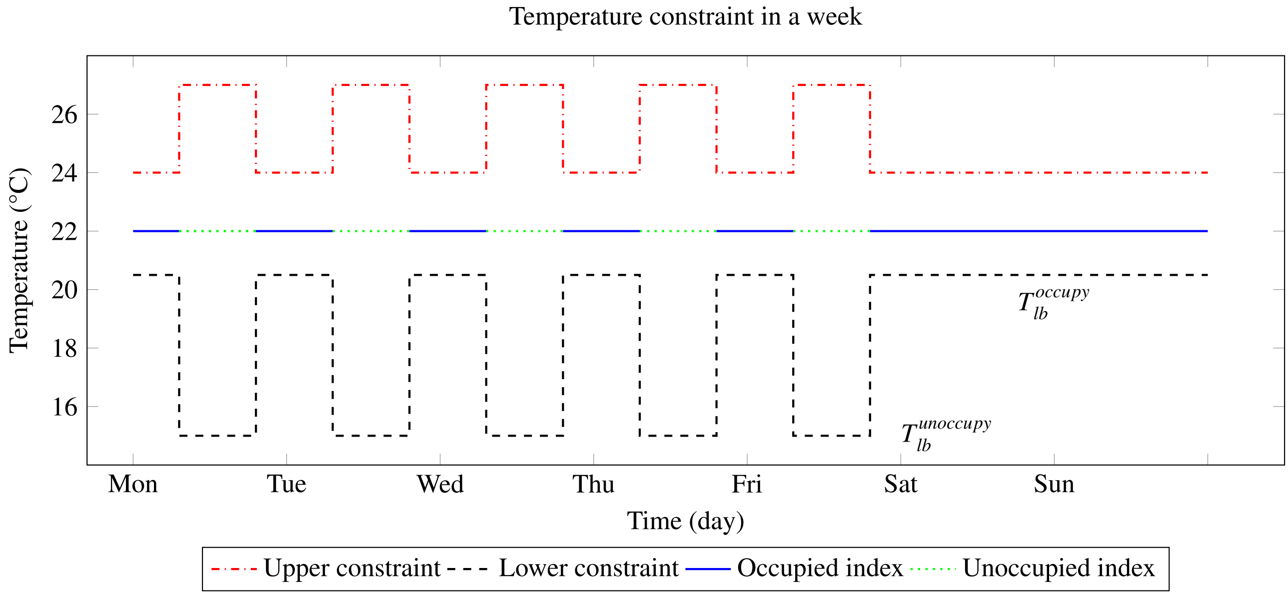

Figure 3: Temperature constraints illustration

Table 2: Approximation methods to include MOP issue in the MPC

Approximation Case	**Details**
MIQP MPC	$\mathrm{U} = \{(u, P_{elec}) \quad \vert \quad 0 \leq u \leq u_{max} * \alpha, \alpha \in \{0, 1\}, P_{elec} = \phi \cdot u + \gamma\}$ $u_{mpc} = mask(u) = u$
Simplified MPC	$\mathrm{U} = \{(u, P_{elec}) \quad \vert \quad 0 \leq u \leq u_{max}, P_{elec} = \phi \cdot u + \gamma\}$ $u_{mpc} = mask(u) = 0 \quad if \quad u < u_{low} \quad else \quad u$

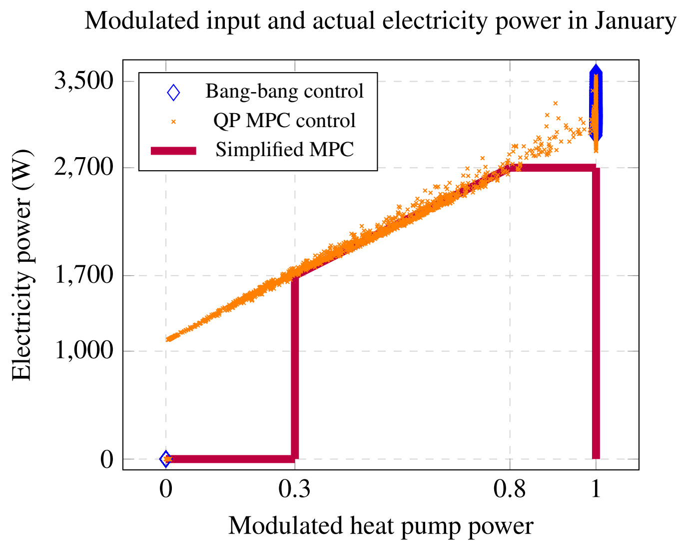

Figure 4: Minimum operating power illustration and concept of the Simplified MPC

MOP problem formulation using the MIQP MPC approximation is referred to as MIQP MPC in the following paper.

As a MIQP problem is computationally expensive and is challenging to be solved by open-source solvers like SCIP [46], especially on low-cost commercial chips. To generalize controllers for wide-spread households, in this case study, we propose another approximation method called Simplified MPC, as illustrated in Fig. 4 and Table. 2. In order to circumvent the issue of minimum operating power, we have applied a mask to the MPC. The lower bound of the mask solves the power issue, while the upper bound of the mask limits the peak power used to decrease the peak power penalty in certain DSM programs, as well as to reduce the overall energy used. Both bounds are critical to the Simplified MPC performance and are to be tuned by our optimization framework. This approach eliminates small input values, avoids system operating at a minimum power, and keeps the MPC as a quadratic programming problem, making it affordable for typical households. Similarly, the MOP problem formulation using the Simplified MPC approximation is referred to as Simplified MPC in the following paper.

Complexity Comparison In this study, we formulated the MPC problem with the CVXPY package [47] and solved it using the MOSEK [48] and SCIP solvers [46]. MOSEK is a commercial solver that is more powerful than the free solver SCIP. We primarily utilized the MOSEK solver, but the SCIP solver was used to illustrate the advantages of Simplified MPC over the MIQP MPC. Subsequently, under the *ddd* pricing case in Table. 5, we compared the average simulation time per step in January as shown in Table. 3. For the simulations in the table, QP and MIQP MPC formulations as mentioned in the previous sections are used with a horizon of 36, a 10th-order linear data-driven model, one-dimensional state, and three-dimensional input. Total simulation time is one month and the control resolution is 15 minutes.

Most simulations in this study were conducted on a powerful computing cluster (Cluster) with 128 GB RAM. To highlight the impractical nature of commercial use for MIQP MPC in building control, we also ran simulations on a personal computer (PC) with 16 GB of RAM, which has less memory than the computing cluster but can still be better than a low-cost chip. Results indicate that solving MIQP is more time-consuming than solving MIQP for both MOSEK and SCIP. It is noteworthy that solving the MIQP using SCIP on a PC can become unresponsive (use up all available RAM) at certain steps for extended periods. To address this, it is necessary to limit the solving time at each step, albeit at the cost of obtaining a lower-quality solution compared to the unrestricted case. In this context, the Simplified MPC is clearly a better choice than a MIQP MPC if they have similar performance.

Table 3: Average time for solving one step on three runs for January

Case	**Average solving time [sec]**	
	Cluster	**PC**
MOSEK QP	0.015	0.011
MOSEK MIQP	0.13	0.089
SCIP QP	0.15	0.233
SCIP MIQP	0.80	∞

The comparison again highlights the infeasibility of deploying a complex MIQP MPC controller in general households due to the mandatory use of an expensive commercial solver. In contrast, the Simplified MPC controller can be solved with a free solver, although it is slower than with a commercial solver. However, building management system inputs are typically updated every 15 minutes or longer, providing enough time for a free solver to solve the QP MPC problem.

4.4. Tuning Variables

Four hyperparameters were selected for tuning with the Simplified MPC: T_{lb}^{occupy}, $T_{lb}^{unoccupy}$, u_{max}, and u_{low}. The lower bounds, T_{lb}^{occupy} and $T_{lb}^{unoccupy}$, are particularly significant, as the indoor temperature trajectory tends to align with the lower bounds without a tracking reference in the objective, heavily influencing individual comfort. u_{max} is crucial for limiting the electricity power applied, thus contributing to cost reduction. Lastly, u_{low} addresses the system minimum operating power problem, as discussed in the previous section. The tuning set is presented in Table. 4, and optimal values are selected from the specified ranges.

Table 4: Details of tuning variables for Simplified MPC

Variable	u_{low}	u_{max}	T_{lb}^{occupy}	$T_{lb}^{unoccupy}$
Range	[0, 0.8]	[0.8, 1]	[21, 23]	[15, 18]

4.5. Tuning objective and constraints for CONFIG

Objective Function In this work, we aim to reduce the monthly electricity bill of a household in Belgium, a concern closely tied to energy consumption and public interest. Unlike simply reducing total energy consumption, which is the sum of energy used, reducing electricity bills is more challenging due to the dynamic and nonlinear nature of electricity pricing. To demonstrate the effectiveness of our performance-oriented optimization method for building control, we specifically target electricity cost minimization as the primary objective.

To provide a more realistic approach, we researched real electricity policies implemented in Vlaanderen, Belgium [49]. This region was chosen because its contracts include a capacity tariff (a charge based on the peak power used every 15 minutes during the month), which makes the pricing policy nonlinear and difficult to integrate into controllers. For simplicity, we divided the charges into three components: time-of-use power charges, capacity tariffs, and fixed charges. A total of 12 distinct contracts were used and compared, with the details provided in Table. 5.

For a given electricity contract B, we introduce u_{peak} to be the max peak electricity power used in 15 minutes of a month, p_{elec}^{B} to be the normal electricity price, p_{capa}^{B} to be the capacity tariff, p_{fixed}^{B} to be the fixed charge, u_t to be the electricity power used in step t, N to be the total simulation time step and then the objective of a month for CONFIG algorithm can be defined as Eq. (7).

$$\begin{aligned} h_{0,k} &= C(z(\theta_k, B), B) \\ &= (\sum_{t=0}^{N-1} u_t p_{elec,t}^{B}) + p_{capa}^{B} * u_{peak} + p_{fixed}^{B} \end{aligned} \tag{7}$$

Constraint Function The optimal control of building systems is a constrained problem. Therefore, in this work, in addition to the direct temperature constraints in the controllers, a constraint based on the Predicted Mean Vote (PMV) is introduced to evaluate the actual performance of the controller. PMV is a comfort index developed by P.O. Fanger [50] to assess human thermal sensation in indoor environments. It is widely used in the field of thermal comfort to evaluate how individuals perceive indoor thermal conditions. The PMV index ranges from -3 to +3, with negative values indicating cold conditions, zero representing thermal neutrality, and positive values indicating warm conditions.

In this project, a relaxed yet more abstract constraint on the PMV is implemented. Following the guidance in [51], the PMV value in a new building must remain between -0.5 and 0.5. But in practice, a few violations are allowed, decided by building designers and clients. For the PMV constraint implemented in the CONFIG algorithm, we have introduced a cumulative distribution function (CDF) integrated with the PMV values. For each time step, the PMV value is calculated and after the building simulation, the PMV values are transmitted to the CONFIG algorithm. As shown in Fig. 5, a CDF is implemented to fit the PMV series and it is expected that within the occupied hours, the absolute PMV value at 80% is smaller than 0.5, meaning that PMV remains within the range of -0.5 to 0.5 for at least 80% of the time when occupants are present in the room. For contract B, we introduce PMV_{CDF}^{B} to be the absolute PMV value at 80% during the occupied hours and then the constraint function can be defined as Eq. (8).

$$h_{1,k} = g(z(\theta_k, B)) = PMV_{CDF}^{B} - 0.5 \tag{8}$$

In this research, only one constraint is implemented. How-

Table 5: 12 Different electricity contract prices in Belgium, Vlaanderen

Name	Single [1]	Day and night [2]		Capacity tariff [3]	Fixed charge	Pricing case [4]
		Day	Night			
Easy Dynamic [5]	-	0.307	0.270	3.35	11.2	ddd
(with capacity tariff)	0.297	-	-	3.35	11.2	dds
Easy Dynamic	-	0.329	0.292	-	19.6	dnd
(no capacity tariff)	0.319	-	-	-	19.6	dns
Easy Static Low	-	0.278	0.253	3.35	11.2	sdd
(with capacity tariff)	0.270	-	-	3.35	11.2	sds
Easy Static Low	-	0.300	0.275	-	19.6	snd
(no capacity tariff)	0.392	-	-	-	19.6	sns
Easy Static High [6]	-	0.307	0.270	3.35	11.2	sdd
(with capacity tariff)	0.297	-	-	3.35	11.2	sds
Easy Static High	-	0.329	0.292	-	19.6	snd1 [6]
(no capacity tariff)	0.319	-	-	-	19.6	sns1

1 Unit: For Single and Day and Night, the unit is €/kWh. For Capacity tariff, the unit is €/kW/month. For Fixed charge, the unit is €/month. The total monthly electricity bill is: (Single or Day and Night)× time of use power + Capacity tariff × peak power per month + Fixed charge.
2 Day time: 7:00 to 22:00, Monday to Friday; Night time is from 22:00 to 7:00, Monday to Friday, and both weekends
3 A charge based on the peak power used every 15 minutes anytime during the month.
4 Composed of three letters: First:‘d’-dynamic, ‘s’-static; Second: ‘d’-with capacity tariff, ‘n’-no capacity tariff; Third:‘d’-day and night, ‘s’-single tariff.
5 Dynamic means price for each month is different. The prices shown in the table are for November of 2023. Please find more details from different contracts in [49] .
6 Static price is decided by the month to sign the contract. Therefore, we have chosen 2 static contracts to compare. ’1’ denotes the statics contract with higher price.

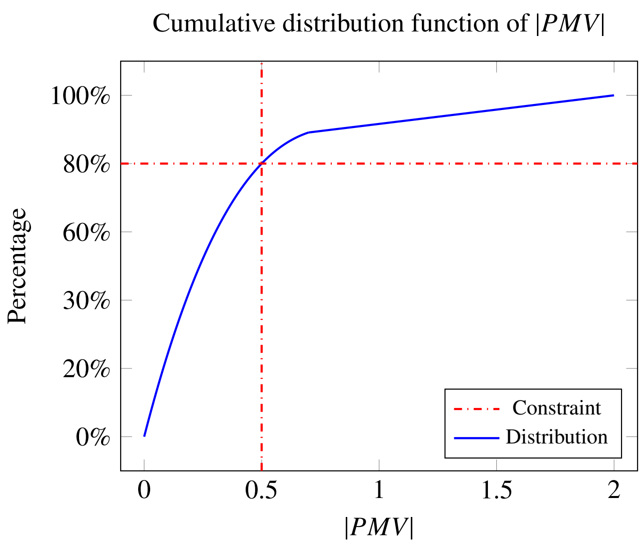

Figure 5: Cumulative distribution function constraint of PMV

ever, both the CONFIG algorithm and the PMV integrated CDF constraint can handle multiple constraints, such as adding a constraint requiring that the absolute PMV value at 50% is smaller than 0.2.

To calculate the PMV, an open-source Python tool package called pythermalcomfort [52] is employed.

5. Case study: offline optimization with BOPTEST

This section outlines the simulation settings and results of a case study for the proposed performance-oriented building MPC controller tuning framework. Firstly, the simulation settings are introduced. Then, results are discussed in two aspects: (1) demonstrating the effects and details of the proposed optimization framework under a normal pricing scenario (ddd, as shown in Table. 5), and (2) conducting a comprehensive comparison of electricity contracts to provide guidance for customers, showcasing the framework’s efficacy in addressing real-world electricity contract selection problems.

5.1. Baseline controllers

This case study employs three baseline controllers: a basic local loop rule-based controller (Baseline), an MIQP MPC controller (MIQP MPC), and an MPC that does not consider system minimum operating power (QP MPC). The rule-based controller (Baseline) is already integrated into the BOPTEST simulation platform and operates using set points, with a higher setpoint (21.2°C) during occupied hours and a lower setpoint (20.5°C) during unoccupied hours. This approach prevents abrupt changes in the indoor temperature, which may not be achievable due to the limitations of the building structure.

The second baseline controller is an MIQP MPC controller (MIQP MPC) as shown in Table. 2. This controller is specifically designed to handle the minimum operating power problem, with hyperparameters set based on expert building system knowledge. There is no constraint on the modulated heat pump input signal, as the mixed-integer nature captures the relationship between the modulated signal and actual electricity power. The lower bound of the indoor temperature for occupied hours is set to 21.5°C

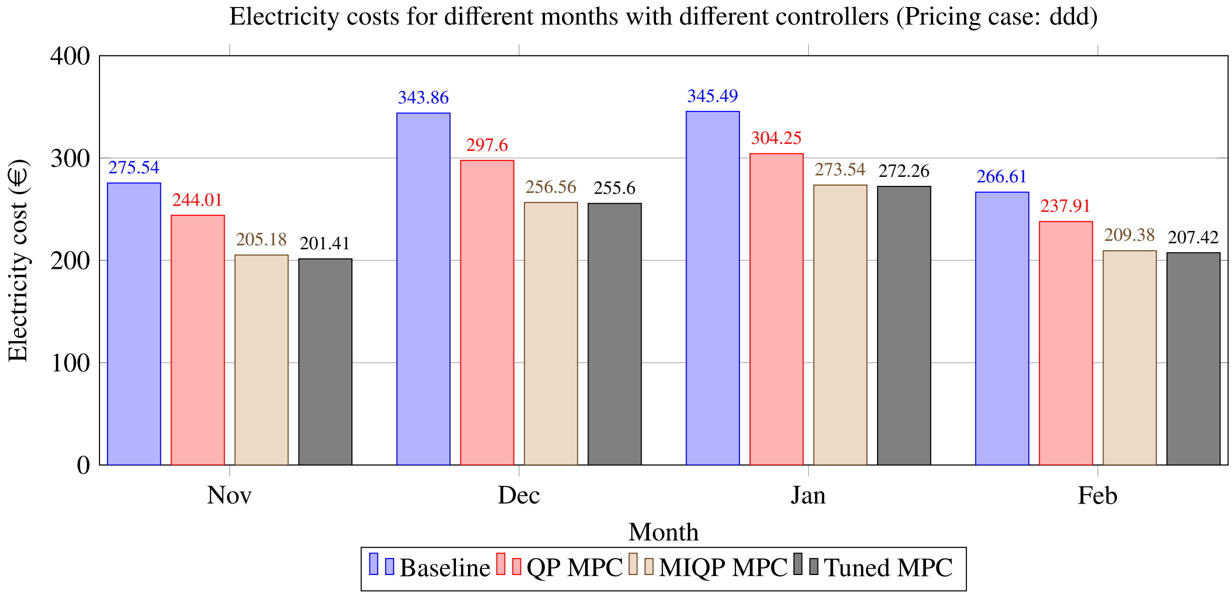

Figure 6: Electricity cost comparison of three different controller. The proposed Tuned MPC can achieve greater performance after tuning in our proposed hyperparameter optimizing framework than the MIQP MPC controller.

and 16°C for unoccupied hours. These hyperparameter values are not precise, as they are not tuned according to real-world performances, but they can still satisfy the PMV constraint while reducing electricity bills to a reasonable extent.

The third baseline controller is a QP MPC without accounting for the minimum operating power issue (QP MPC) although it exists in the simulation. The formulation of the QP MPC follows Eq. (5) and uses the same temperature constraints as the MIQP MPC. It can also be seen as an untuned Simplified MPC with $u_{low} = 0$, $u_{max} = 1$, and randomly set temperature lower bounds. The trajectory difference between the QP MPC and the tuned Simplified MPC stems from hyperparameter tuning.

5.2. Experiments design

To improve MPC controller performance, simulations are run over one-month periods for November, December, January, and February. This duration was chosen to capture the significant weather variation during these months, as the ARX model struggles to handle such complexity effectively.

To address the two outlined objectives, we designed two experiments. In the first experiment, we compared the performance of **the optimized Simplified MPC (Tuned MPC)** and the three baseline controllers. Four hyperparameters were optimized as mentioned in section. 4.4. In the second experiment, we tuned the same hyperparameter set, however, a total number of 12 pricing cases are compared. This required running the optimization process 12 times and comparing the best performance for each pricing case. Finally, a guidance for the local household in a similar scale as shown in Table. 1 was offered.

5.3. Results and discussions

5.3.1. Details of optimization

Firstly, a comparative analysis of the final electricity costs was conducted for the baseline controller, the QP MPC, the computationally intensive MIQP MPC controller, and the tuned Simplified MPC (Tuned MPC) under the same pricing case (ddd as shown in Table. 5), as illustrated in Fig. 6. To show the robustness of our optimization framework, the results for Tuned MPC are averages for four different initial conditions. It is evident that in comparison to the baseline controller, all three MPC controllers significantly reduce the final electricity costs for different months. The cost difference between the baseline and the QP MPC reflects the profit brought by the predictive ability of conventional MPC, while the cost difference between the QP MPC and the Tuned MPC is the profit achieved by hyperparameter tuning. In fact, the hyperparameter tuning contributes to as much cost reduction as the predictive ability of MPC which illustrates the vitality to perform hyperparameter tuning on MPC controllers in building control and the superior effects of our optimization framework.

Besides, the Tuned MPC, in particular, has the potential to reduce these costs by up to 26.90%. For all months, the costs of the Tuned MPC are consistently smaller than those of the MIQP MPC. It can be demonstrated that the proposed Tuned MPC can achieve greater performance after tuning in our proposed hyperparameter optimizing framework than the MIQP MPC controller. However, the computational cost of the Tuned MPC is much lower than that of the MIQP MPC, as demonstrated in Table. 3.

In specific terms, Fig. 7 highlights that the MPC controller's cost savings stem from its superior prediction capabilities, including its enhanced knowledge of temperature constraints and electricity prices compared to the baseline rule-based controller. For the two MPC controllers, Tuned MPC achieves even slightly better performance than the computationally intensive MIQP MPC with its ability to regulate the heat pump input to a specific range. Additionally, the simulation time of the Tuned MPC is nearly 40% less than MIQP MPC as expected in the *complexity*

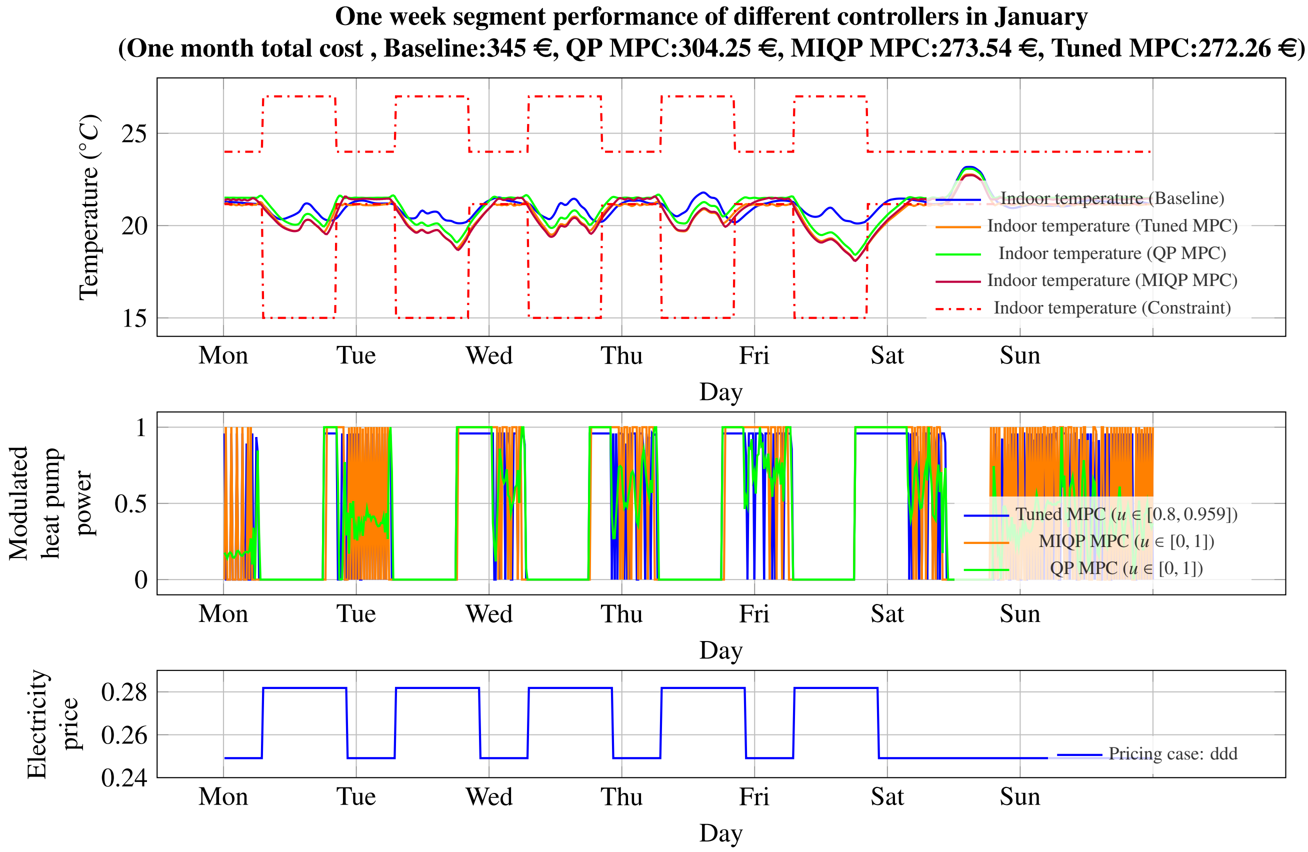

Figure 7: Performance comparison of three different controllers

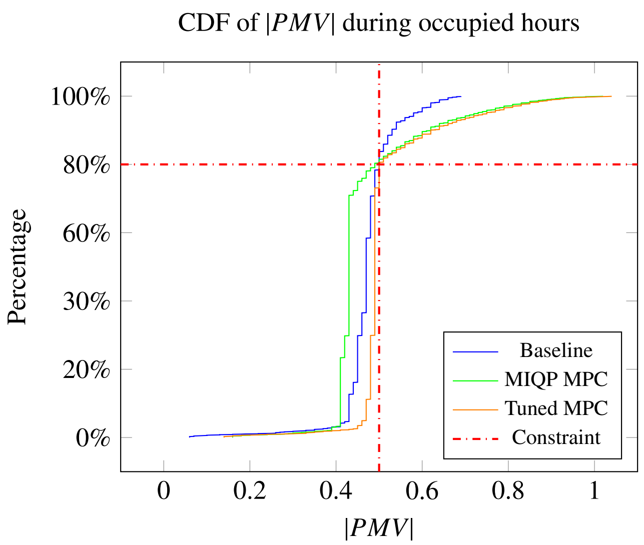

Figure 8: Cumulative distributive function of absolute PMV during occupied hours in January. Constraint: 80% of the absolute PMV values during occupied hours are smaller than 0.5.

comparison part of section. 4.3. While the indoor temperature trajectories of Tuned MPC and MIQP MPC are quite similar, Tuned MPC applies more accurate temperature constraints after optimization, resulting in further cost savings while maintaining comfort constraints. It is notable that the modulated heat pump inputs computed by MIQP MPC and Tuned MPC exhibit a non-continuous, jagged shape. This phenomenon is due to the minimum operating power issue, where using a small modulated heat pump input becomes inefficient, as the power used for heating is only a small fraction of the total electricity consumed.

To clearly show the precise temperature constraints enabled by our proposed optimization framework, we have compared the comfort index CDF of the three controllers as shown in Fig. 8. From the CDF of absolute PMV values during the occupied hours in January, it can be observed that while all three controllers satisfy the comfort constraint (80% of the absolute PMV values during occupied hours are smaller than 0.5), the Tuned MPC is most effective in achieving this result through the precise tuning of temperature constraints and the mask in the Simplified MPC. Overall, with significantly lower commissioning costs in terms of solver and hardware requirements compared to the MIQP MPC, the Tuned MPC achieves comparable or even superior performance.

It should be noted that manually tuning these hyperparameters may seem straightforward, such as lowering the temperature and limiting the heat pump input. However, trial-and-error methods are impractical due to the black-box nature of the PMV comfort constraint, making it difficult to satisfy precisely. We have also plotted the posterior means in Fig. 9 where a 4-dimensional sample set are sliced into two 2-dimensional sets for presentation purpose. Background color represents the level sets of the posterior mean for the objective and constraint function, respectively. To be noted, the posterior mean of the two variables is computed when the other two variables are fixed at optimal values.

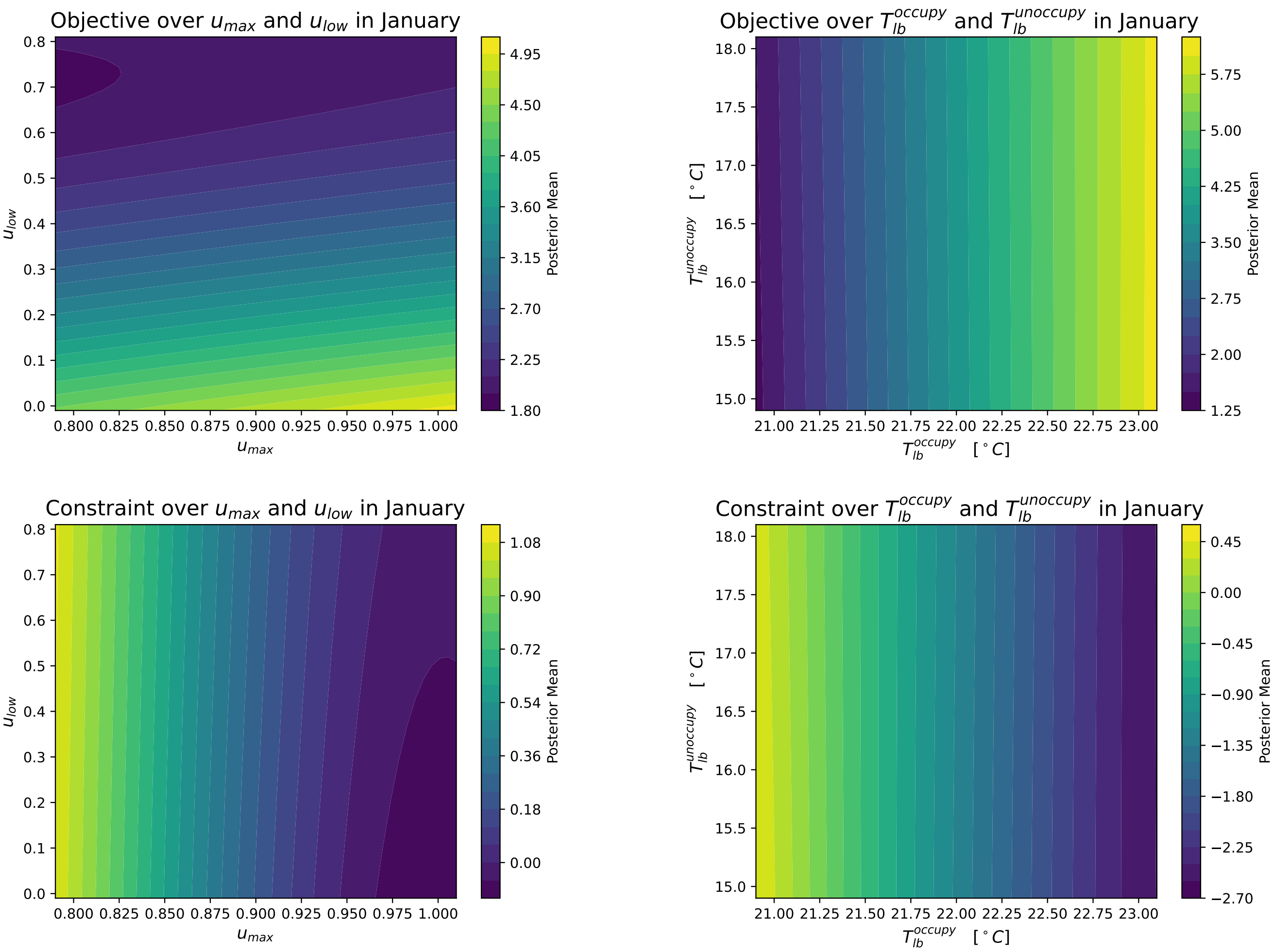

Figure 9: Level set plots from a 4-dimensional space sliced to two 2-dimensional spaces. The color represents the level sets of the posterior mean for the objective and constraint function, respectively. For each plot, the left two dimensions are fixed at their optimal values.

Empirically, feasibility is primarily influenced by T_{lb}^{occupy} with improved feasibility observed when the T_{lb}^{occupy} and $T_{lb}^{unoccupy}$ are higher, u_{low} is smaller and u_{max} is larger. However, as the optimization problem exists in 4 dimensions, there is no clearly defined feasible region when viewed in 2D. In fact, as shown in Fig. 10, a single point in the 2D projection may appear feasible or infeasible depending on the values of the other two dimensions. This interdependence in feasibility also helps to explain the discontinuity of the feasible and infeasible points in the projection. This complexity further highlights the need for an automatic tuning framework to reduce manual effort, which is often complex, time-consuming, and prone to suboptimal outcomes.

5.3.2. Comparison of electricity contracts

After validating the proposed performance-oriented MPC controller tuning method in building control, we analyzed 12 different contracts as mentioned in Table. 5. We hope our performance oriented MPC controller tuning framework for building control will serve as a guide for the customers in Belgium to better choose an electricity contract, i.e. a contract that costs the least.

After tuning the Simplified MPC controller for each contract and each month, as shown in Table. 6, it is evident that choosing a proper electricity bill is vital as it could help customers save up to 53.70 euros a month and that the best bills are reduced up to 20.18% compared with the worst cases. The results again illustrate the significance of choosing a proper electricity contract. To be noted, all results for Tuned MPC reflect the optimal outcomes for different contracts respectively. And the different costs between Tuned MPC and QP MPC illustrate the vitality of hyperparameter tuning for MPC in building control.

From the Tuned MPC results, we can also indicate that it would be beneficial if the customers can choose a different contract for each month, however, it is impractical as there has been a minimum of one year duration for all contracts. Therefore, we need to offer a more general guidance for the customers. We have found that for both dynamic and fixed tariff contracts (each 4 rows), the day and night tariff with capacity tariff is the best combination. Then we have plotted the contracts with day and night tariff and capacity tariff combination, namely ddd (dynamic tariff, day and night tariff with capacity tariff), sdd (lower fixed tariff, day and night tariff with capacity tariff) and sdd1 (higher fixed tariff, day and night tariff with capacity tariff)

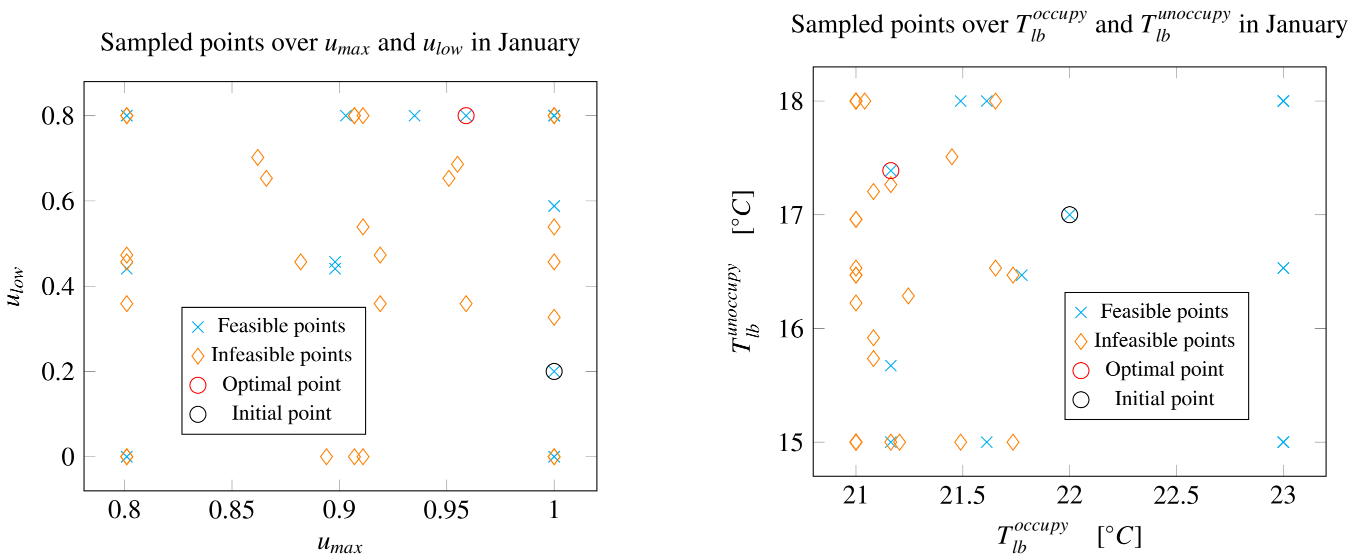

Figure 10: Sampled points from a single optimization process, projected from a 4-dimensional space onto two 2-dimensional subspaces. A point in the 2D plots may appear feasible or infeasible depending on the fixed values of the other two dimensions (e.g., the lower-left corner point in the left plot).

Table 6: Optimized electricity bills under different pricing methods for different months

Pricing case	Electricity bills (€/month)							
	November		December		January		February	
	Tuned MPC	QP MPC	Tuned MPC	QP MPC	Tuned MPC	QP MPC	Tuned MPC	QP MPC
ddd	201.41	244.01	255.60	297.60	272.26	304.25	**207.42**	237.91
dds	211.96	259.16	269.05	314.89	284.96	322.41	217.58	251.00
dnd	212.13	256.28	270.84	316.13	288.37	324.73	224.70	254.03
dns	223.57	271.83	284.22	333.76	302.88	342.90	230.47	267.11
sdd	**190.22**	228.97	**248.95**	290.12	**272.14**	328.13	222.62	252.92
sds	195.08	237.42	257.19	301.15	282.33	348.81	227.22	262.68
snd	201.82	242.00	266.43	308.82	289.97	348.59	235.59	269.01
sns	205.11	251.12	272.28	319.95	299.85	369.31	239.77	278.86
sdd1	201.31	243.78	267.59	310.39	291.28	328.13	236.75	270.37
sds1	212.38	259.22	280.53	329.10	308.17	348.59	246.53	286.75
snd1	213.54	256.22	281.56	329.24	310.13	348.81	246.65	286.35
sns1	**222.72**	271.89	**296.23**	347.82	**325.84**	369.31	**259.86**	302.81
SP[1]	33.35	-	47.28	-	53.70	-	52.44	-
SR[2]	14.94%	-	15.96%	-	16.48%	-	20.18%	-

[1] SP: Saving potential, worst case bill - best case bill, unit: €/month.
[2] SR: Saving ratio, (worst case bill - best case bill)/worst case bill, unit:1.

as illustrated in Fig. 11. For February, ddd is the best while sdd is the best for the other months. It seems that sdd is the optimal choice when choosing a electricity contract, however it is contingent upon the electricity price being sufficiently low when signing the contract. If electricity prices are high, the final cost of electricity will be less favorable than that of the dynamic option, similar to the sdd1. Therefore, given the uncertainty surrounding the trajectory of electricity prices, customers are recommended to consider selecting the ddd option.

While the QP MPC may also suggest similar contracts, it can yield suboptimal recommendations in more complex scenarios. For instance, in the presence of electrical vehicle charging, the resulting high peak demand can make capacity charges a significant factor. In such cases, a contract with a high capacity tariff but lower time-of-use rates may seem attractive for QP MPC as it does not account for peak demand charges, which are particularly relevant in commercial settings. In contrast, the Tuned MPC is able to provide more appropriate recommendations even under such challenging conditions as the total cost including the capacity charge is set as the objective for the optimization framework.

6. Conclusion

In this paper, we addressed two key challenges: selecting the most cost-effective electricity contract from various options and improving the suboptimal performance of conventional building MPC controller designs. To tackle these issues, we proposed a performance-oriented optimization framework using the ad-

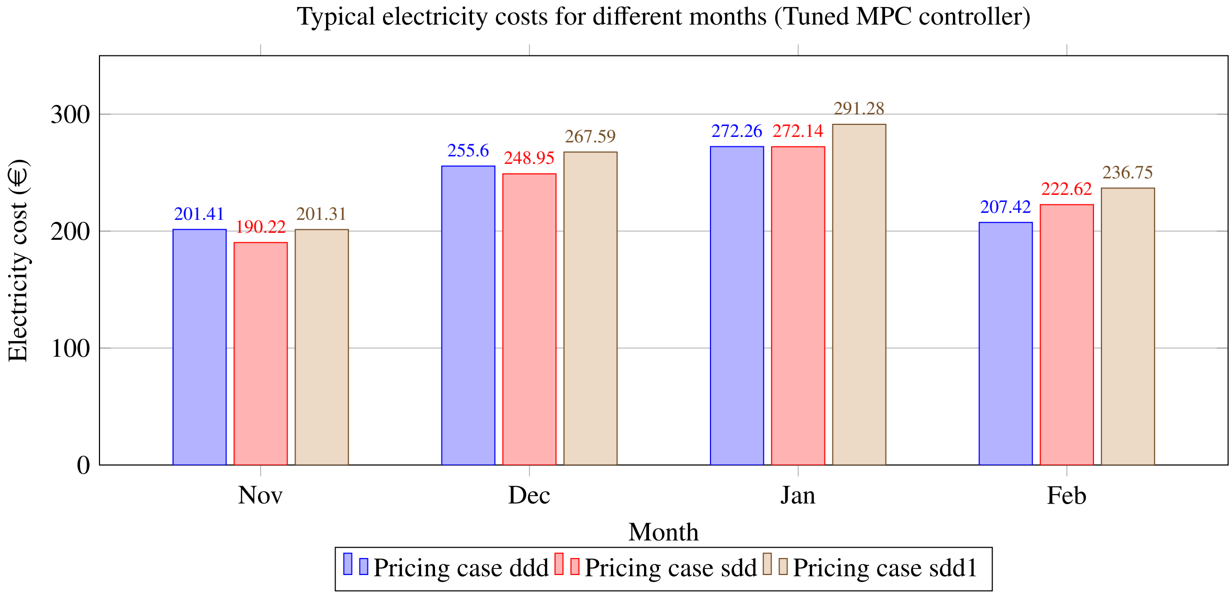

Figure 11: Electricity costs for four months with different pricing policies

vanced constrained black-box optimization technique, CONFIG. Leveraging a digital twin like the BOPTEST simulation platform, offline optimization was performed to identify the optimal set of hyperparameters. This process minimizes the objective value while ensuring compliance with the black-box comfort constraints.

A case study on a household in Belgium demonstrates that a simple MPC controller, when properly tuned, can match the performance of a computationally intensive one. Simulations show that optimized MPC controllers can reduce monthly electricity bills by up to 26.90% during heating months while maintaining strict black-box constraints. Additionally, our framework effectively addresses the economic electricity contract selection problem, with the most cost-effective contract yielding a 20.18% savings compared to the least favorable option.

While the framework effectively addresses real-world issues, it has only been tested through offline optimization experiments in this paper. Adapting the framework for online optimization presents an intriguing direction for future work. In offline optimization, performance metrics such as the monthly electricity bill can be readily calculated, enabling a comprehensive evaluation of the framework's effectiveness under various scenarios. In contrast, real-time online optimization introduces additional challenges, as metrics like the monthly electricity bill remain unknown and must be estimated or predicted on the fly. Addressing these challenges would enhance the framework's applicability and scalability for dynamic, real-world implementations.

Acknowledgements

This research was supported by the Swiss National Science Foundation under NCCR Automation, grant agreement 51NF40_180545.

References

[1] U. N. E. Programme, 2022 global status report for buildings and construction: Towards a zero-emission, efficient and resilient buildings and construction sector (2022-11).

[2] M. Davies, Benchmarking commercial building energy use per square foot, Altenergymag.com (Jun. 8, 2019).

[3] C. Eid, E. Koliou, M. Valles, J. Reneses, R. Hakvoort, Time-based pricing and electricity demand response: Existing barriers and next steps, Utilities Policy 40 (2016) 15–25. doi:https://doi.org/10.1016/j.jup.2016.04.001.

[4] ENGIE, Engie website guidance, https://www.engie.be/nl/elektriciteit-gas/, accessed: 2024-11-27.

[5] selectandswitch, Select and switch website, https://selectandswitch.com.au/, accessed: 2024-11-27.

[6] Y. Cui, Z. Zhu, X. Zhao, Z. Li, Energy schedule setting based on clustering algorithm and pattern recognition for non-residential buildings electricity energy consumption, Sustainability 15 (11) (2023). doi:10.3390/su15118750.

[7] S. Wang, L. Kong, C. Liu, G. Cai, Mpc-based energy optimization and regulation for zero-carbon energy supply building, International Journal of Hydrogen Energy 82 (2024) 1196–1210. doi:https://doi.org/10.1016/j.ijhydene.2024.07.397.

[8] S. Yang, M. P. Wan, W. Chen, B. F. Ng, S. Dubey, Model predictive control with adaptive machine-learning-based model for building energy efficiency and comfort optimization, Applied Energy 271 (2020) 115147. doi:https://doi.org/10.1016/j.apenergy.2020.115147.

[9] P. C. Tabares-Velasco, A. Speake, M. Harris, A. Newman, T. Vincent, M. Lanahan, A modeling framework for optimization-based control of a residential building thermostat for time-of-use pricing, Applied Energy 242 (2019) 1346–1357. doi:https://doi.org/10.1016/j.apenergy.2019.01.241.

[10] N. T. Mbungu, R. M. Naidoo, R. Bansal, Real-time electricity pricing: Tou-mpc based energy management for commercial buildings, Energy Procedia 105 (2017) 3419–3424, 8th International Conference on Applied Energy, ICAE2016, 8-11 October 2016, Beijing, China. doi:https://doi.org/10.1016/j.egypro.2017.03.781.

[11] F. Oldewurtel, A. Ulbig, A. Parisio, G. Andersson, M. Morari, Reducing peak electricity demand in building climate control using real-time pricing and model predictive control, in: 49th IEEE Conference on Decision and Control (CDC), 2010, pp. 1927–1932. doi:10.1109/CDC.2010.5717458.

[12] S. Yang, H. Oliver Gao, F. You, Model predictive control for demand- and market-responsive building energy management by leveraging active latent heat storage, Applied Energy 327 (2022) 120054. doi:https://doi.org/10.1016/j.apenergy.2022.120054.

[13] G. Serale, M. Fiorentini, A. Capozzoli, D. Bernardini, A. Bemporad, Model predictive control (mpc) for enhancing building and hvac system energy efficiency: Problem formulation, applications and opportunities,

Energies 11 (3) (2018). doi:10.3390/en11030631.

[14] Y. Pan, M. Zhu, Y. Lv, Y. Yang, Y. Liang, R. Yin, Y. Yang, X. Jia, X. Wang, F. Zeng, S. Huang, D. Hou, L. Xu, R. Yin, X. Yuan, Building energy simulation and its application for building performance optimization: A review of methods, tools, and case studies, Advances in Applied Energy 10 (2023) 100135. doi:https://doi.org/10.1016/j.adapen.2023.100135.

[15] H. Doddi, S. Talukdar, D. Deka, M. Salapaka, Data-driven identification of a thermal network in multi-zone building (2018). arXiv:1810.07400.

[16] Z. Wang, Y. Chen, Y. Li, Development of rc model for thermal dynamic analysis of buildings through model structure simplification, Energy and Buildings 195 (2019) 51–67. doi:https://doi.org/10.1016/j.enbuild.2019.04.042.

[17] Y. Lian, J. Shi, M. Koch, C. N. Jones, Adaptive robust data-driven building control via bilevel reformulation: An experimental result, IEEE Transactions on Control Systems Technology 31 (6) (2023) 2420–2436. doi:10.1109/TCST.2023.3259641.

[18] F. Massa Gray, M. Schmidt, Thermal building modelling using gaussian processes, Energy and Buildings 119 (2016) 119–128. doi:https://doi.org/10.1016/j.enbuild.2016.02.004.

[19] C. Fan, J. Wang, W. Gang, S. Li, Assessment of deep recurrent neural network-based strategies for short-term building energy predictions, Applied Energy 236 (2019) 700–710. doi:https://doi.org/10.1016/j.apenergy.2018.12.004.

[20] J. Hu, W. Zheng, S. Zhang, H. Li, Z. Liu, G. Zhang, X. Yang, Thermal load prediction and operation optimization of office building with a zone-level artificial neural network and rule-based control, Applied Energy 300 (2021) 117429. doi:https://doi.org/10.1016/j.apenergy.2021.117429.

[21] S. Yang, H. O. Gao, F. You, Integrated optimization in operations control and systems design for carbon emission reduction in building electrification with distributed energy resources, Advances in Applied Energy (2023) 100144doi:https://doi.org/10.1016/j.adapen.2023.100144.

[22] F. Oldewurtel, A. Parisio, C. Jones, M. Morari, D. Gyalistras, M. Gwerder, V. Stauch, B. Lehmann, K. Wirth, Energy efficient building climate control using stochastic model predictive control and weather predictions, Proceedings of the 2010 American Control Conference, ACC 2010 (2010) 5100 – 5105doi:10.1109/ACC.2010.5530680.

[23] J. Joe, P. Karava, A model predictive control strategy to optimize the performance of radiant floor heating and cooling systems in office buildings, Applied Energy 245 (2019) 65–77. doi:https://doi.org/10.1016/j.apenergy.2019.03.209.

[24] A. Mishra, H. R. Lone, A. Mishra, Decode: Data-driven energy consumption prediction leveraging historical data and environmental factors in buildings, Energy and Buildings 307 (2024) 113950. doi:10.1016/j.enbuild.2024.113950.

[25] T. Xiao, F. You, Building thermal modeling and model predictive control with physically consistent deep learning for decarbonization and energy optimization, Applied Energy 342 (2023) 121165. doi:https://doi.org/10.1016/j.apenergy.2023.121165.

[26] Q. Zhang, L. Wang, W. Xu, H. Su, L. Xie, Nonlinear sparse variational bayesian learning based model predictive control with application to pemfc temperature control (2024). arXiv:2404.09519.

[27] A. Mugnini, G. Coccia, F. Polonara, A. Arteconi, Performance assessment of data-driven and physical-based models to predict building energy demand in model predictive controls, Energies 13 (12) (2020). doi:10.3390/en13123125.

[28] W. Xu, B. Svetozarevic, L. Di Natale, P. Heer, C. N. Jones, Data-driven adaptive building thermal controller tuning with constraints: A primal–dual contextual bayesian optimization approach, Applied Energy 358 (2024) 122493. doi:https://doi.org/10.1016/j.apenergy.2023.122493.

[29] X. Lin, Q. Guo, D. Yuan, M. Gao, Bayesian optimization framework for hvac system control, Buildings 13 (2) (2023). doi:10.3390/buildings13020314.

[30] H. Ren, D. ce Gao, Z. Ma, S. Zhang, Y. Sun, Data-driven surrogate optimization for deploying heterogeneous multi-energy storage to improve demand response performance at building cluster level, Applied Energy 356 (2024) 122312. doi:https://doi.org/10.1016/j.apenergy.2023.122312.

[31] Z. Deng, M. Chen, H. Wang, Q. Chen, Performance-oriented model learning and model predictive control for pemfc air supply system, International Journal of Hydrogen Energy 64 (2024) 339–348. doi:https://doi.org/10.1016/j.ijhydene.2024.01.351.

[32] N. A. Choksi, J. A. Paulson, Simulation-based integrated design and control with embedded mixed-integer mpc using constrained bayesian optimization, in: 2021 American Control Conference (ACC), 2021, pp. 2114–2120. doi:10.23919/ACC50511.2021.9482646.

[33] Q. Lu, R. Kumar, V. M. Zavala, Mpc controller tuning using bayesian optimization techniques (2021). arXiv:2009.14175.

[34] Q. Lu, L. D. González, R. Kumar, V. M. Zavala, Bayesian optimization with reference models: A case study in mpc for hvac central plants, Computers & Chemical Engineering 154 (2021) 107491. doi:https://doi.org/10.1016/j.compchemeng.2021.107491.

[35] W. Xu, Y. Jiang, B. Svetozarevic, C. N. Jones, Constrained efficient global optimization of expensive black-box functions (2025). arXiv:2211.00162.

[36] M. W. Grieves, J. H. Vickers, Digital twin: Mitigating unpredictable, undesirable emergent behavior in complex systems, 2017.

[37] D. Blum, J. Arroyo, S. Huang, J. Drgoňa, F. Jorissen, H. T. Walnum, Y. Chen, K. Benne, D. Vrabie, M. Wetter, L. Helsen, Building optimization testing framework (boptest) for simulation-based benchmarking of control strategies in buildings, Journal of Building Performance Simulation 14 (5) (2021) 586–610. arXiv:https://doi.org/10.1080/19401493.2021.1986574, doi:10.1080/19401493.2021.1986574.

[38] B. Dong, K. P. Lam, A real-time model predictive control for building heating and cooling systems based on the occupancy behavior pattern detection and local weather forecasting 7 (1) 89–106. doi:10.1007/s12273-013-0142-7.

[39] J. Shi, Y. Lian, C. Salzmann, C. N. Jones, Adaptive data-driven prediction in a building control hierarchy: A case study of demand response in switzerland, Energy and Buildings 333 (2025) 115498. doi:10.1016/j.enbuild.2025.115498.

[40] D. Zhou, Q. Hu, C. J. Tomlin, Model comparison of a data-driven and a physical model for simulating hvac systems (2016). arXiv:1603.05951.

[41] J. Ke, Y. Qin, B. Wang, S. Yang, H. Wu, H. Yang, X. Zhao, Data-driven predictive control of building energy consumption under the iot architecture, Wireless Communications and Mobile Computing 2020 (1) (2020) 8849541. doi:https://doi.org/10.1155/2020/8849541.

[42] J. Drgoňa, J. Arroyo, I. Cupeiro Figueroa, D. Blum, K. Arendt, D. Kim, E. P. Ollé, J. Oravec, M. Wetter, D. L. Vrabie, L. Helsen, All you need to know about model predictive control for buildings, Annual Reviews in Control 50 (2020) 190–232. doi:https://doi.org/10.1016/j.arcontrol.2020.09.001.

[43] F. Bünning, B. Huber, A. Schalbetter, A. Aboudonia, M. Hudoba de Badyn, P. Heer, R. S. Smith, J. Lygeros, Physics-informed linear regression is competitive with two machine learning methods in residential building MPC, Appl. Energy 310 (118491) (2022) 118491.

[44] F. Gauthier-Clerc, H. Le Capitaine, F. Claveau, P. Chevrel, Comparing neural network and linear models in economic mpc: Insights from boptest for building temperature control, in: 2024 European Control Conference (ECC), 2024, pp. 2518–2525. doi:10.23919/ECC64448.2024.10590813.

[45] D. Blum, J. Arroyo, S. Huang, J. Drgoňa, F. Jorissen, H. T. Walnum, Y. Chen, K. Benne, D. Vrabie, M. Wetter, L. H. and, Building optimization testing framework (boptest) for simulation-based benchmarking of control strategies in buildings, Journal of Building Performance Simulation 14 (5) (2021) 586–610. doi:10.1080/19401493.2021.1986574.

[46] S. Bolusani, M. Besançon, K. Bestuzheva, A. Chmiela, J. Dionísio, T. Donkiewicz, J. van Doornmalen, L. Eifler, M. Ghannam, A. Gleixner, C. Graczyk, K. Halbig, I. Hedtke, A. Hoen, C. Hojny, R. van der Hulst, D. Kamp, T. Koch, K. Kofler, J. Lentz, J. Manns, G. Mexi, E. Mühmer, M. E. Pfetsch, F. Schlösser, F. Serrano, Y. Shinano, M. Turner, S. Vigerske, D. Weninger, L. Xu, The SCIP Optimization Suite 9.0, Technical report, Optimization Online (February 2024).

[47] S. Diamond, S. Boyd, CVXPY: A Python-embedded modeling language for convex optimization, Journal of Machine Learning Research 17 (83) (2016) 1–5.

[48] MOSEK ApS, MOSEK Optimization Tools, https://www.mosek.com/, version 10.1.17 (2023).

[49] Engie website electricity contracts, https://www.engie.be/nl/energie/elektriciteit-gas/prijzen-voorwaarden/, accessed:

2024-03-22 (2024).
[50] P. O. Fanger, Thermal comfort: Analysis and applications in environmental engineering, Danish Technical Press, 1970.
[51] En 15251:2007, indoor environmental input parameters for design and assessment of energy performance of buildings addressing indoor air quality, thermal environment, lighting and acoustics.
[52] F. Tartarini, S. Schiavon, pythermalcomfort: A python package for thermal comfort research, SoftwareX 12 (100578) (2020) 100578.